PARAMETER STUDY FOR LORAWAN IN AN URBAN ENVIRONMENT

Laura Isabella Correa Rubio

Supervisor at UPV: María de Diego Antón

Supervisor at TUHH: Andreas Timm-Giel

Final Bachelor Thesis submitted as a partial requirement to obtain the Bachelor's Degree in Telecommunications Technologies and Services Engineering.

Developed under the Erasmus+ program at the Hamburg University of Technology.

Academic Year 2019-20

April 2021

Abstract

LoRa is an LPWAN technology present in many different IoT applications, although specific information about its performance is not largely available. Therefore, it is important to know what Key Performance Indicators (KPIs) can be used and what parameters affect these KPIs, and how. To achieve this, in this thesis a literature review of LoRa-based IoT applications has been done, allowing us to identify power consumption, delay, and packet-loss ratio as the main KPIs. Three different experimental scenarios in the city of Bremen, one static and two mobile, were used to evaluate the identified KPIs, changing the values of the parameters influencing them. These are Spreading Factor (SF), Class, range, and payload. For higher Spreading Factors (SFs), higher delay and lower packet-loss ratios are obtained. Also, a higher payload value results in higher delay. The packet loss ratio also increases with longer distances between the node and the gateway. Anyhow, shorter distances in more dense areas also show a higher packet loss ratio. The maximum reachable distance of the node-gateway in our experiments was around 7 km, a quite high value for an urban environment.

Resumen

LoRa es una tecnología LPWAN presente en numerosas aplicaciones IoT, aunque información específica sobre su funcionamiento no está disponible en gran medida. Por tanto, es importante saber qué KPIs la definen qué parámetros afectan a estas KPIs y cómo. Para lograr esto, en este TFG se ha realizado una revisión bibliográfica de aplicaciones IoT basadas en LoRa, permitiéndonos identificar la potencia consumida, retardo y la ratio de pérdida de paquetes como las KPIs objeto de estudio. Tres escenarios experimentales en la ciudad de Bremen, uno estático y dos móviles, han sido utilizados para examinar estas KPIs, cambiando los valores de los parámetros que influyen en ellas. Estos son: Spreading Factor (SF), clase, rango y payload. Se ha podido corroborar que para valores más altos de SF se obtiene mayor retardo y una ratio de pérdida de paquetes más alto. Además, un payload más grande resulta en un retardo mayor. Por último, para distancias más largas entre nodo y antena receptora, la pérdida de paquetes también aumenta. La máxima distancia nodo-gateway hallada en nuestros experimentos es de más de 7 km, un valor bastante elevado para un entorno urbano.

List of Tables

List of Figures

Table of Contents

Introduction

When talking about smart buildings, factories or hospitals, everybody immediately thinks about IoT. Internet of Things is the (not so) new technological advance that promises to connect everything and systematize any procedure at hand, making living more comfortable, secure, and reliable. At least, that is what, reading outside the box, people get to imagine. But what is there behind IoT? What are the aims of its use? IoT is usually defined as the interconnection of devices capable of receiving and sending data through the Internet. Therefore, there exist the goal of finding the optimal way of implementing this interconnection. Usually, this refers to speed, reliability, power consumption, robustness, and range. Among the different options available, Low Power Wide Area Networks (LPWANs) are one of the main focuses.

This type of technology aims to provide a wide range of communication with low power consumption, which is greatly interesting for IoT deployments. LoRa, pertaining to this group, is a relatively new technology offering a great performance on a low power consumption basis. Anyhow, there exist a good number of papers referring to real-life deployments using LoRa as their communication technology, giving a broad overview of what characteristics of these applications LoRa can cover, and what values the configuration parameters of LoRa take in real-life scenarios. This motivated us to test how, depending on the values given to certain parameters of LoRa, its performance changed. Therefore, the aim of this study is, in the first place, to do an extensive literature survey of LoRa-based IoT applications to determine the KPIs of this technology and the parameters that affect them. Later, through different experimental scenarios, we are willing to test in what measure these parameters and the changes introduced in them, affect the identified KPIs.

In this document, the LoRa technology will be briefly introduced in chapter 1. In chapter 2, a short review of previous works will be given, including a classification of the parameters used for different applications. The KPIs to be tested and the parameters affecting them will also be identified. In chapter 3, our experimental proposal will be explained, as well as the results obtained, and the conclusions extracted from them. In chapter 4 we will summarize the formulas found to describe parts of LoRa behaviour as well as a general explanation of the mathematical path-loss model for urban environments, which fits our testing environment. Finally, the conclusions will be discussed in chapter 5.

Chapter 1: LoRa technology

LoRa, short for Long Range, is a wireless technology that allows small package transmission over long distances with low power consumption. This technology is based on Chirp Spread Spectrum (CSS) with Forward Error Correction (FEC) [1], which in great measure increases the communication range in comparison to Frequency Shifting Keying (FSK) while maintaining its same low power characteristics [27].

LoRa's physical Layer operates over any Media Access Control (MAC) [1], but the one standardized by the LoRa Alliance is the so called LoRaWAN, an open-source protocol [24].

The LoRaWAN network has a star topology, where multiple end nodes are connected to a single Gateway (GW), communicating through it instead of one directly with each other.

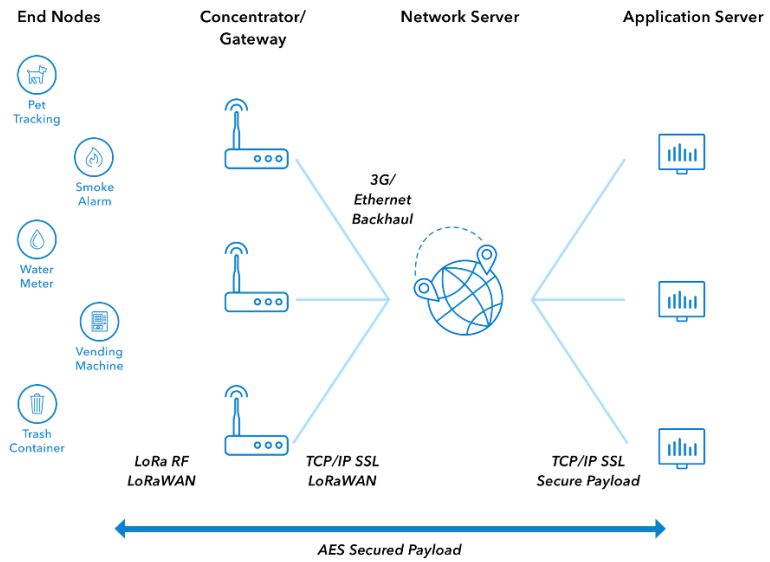

Fig. 1: LoRaWAN Topology [29]

1.1 Classes

When talking about LoRaWAN, we find three different classes: class A, B or C. Depending on the requirements the application to be implemented has, one of these classes is used. [23].

The following characteristics apply [24]:

- **Class A**: It is the most basic of the three available classes. In this configuration, the end node can send a package to the GW. After this uplink transmission ends, the end node opens two receive windows in case there is some downlink traffic.

  These two downlink receive windows open 1 and 2 seconds after the uplink transmission finishes. Both windows, one or none can be used.

  If the first window is used, the downlink transmission will occupy the same channel as the uplink transmission. In case the second window is used, then a fixed channel with fixed SF will be set for the transmission.

  After the downlink transmission happens, it waits for an uplink transmission to take place. Since most of the time they are inactive, Class A devices are the least power consuming.

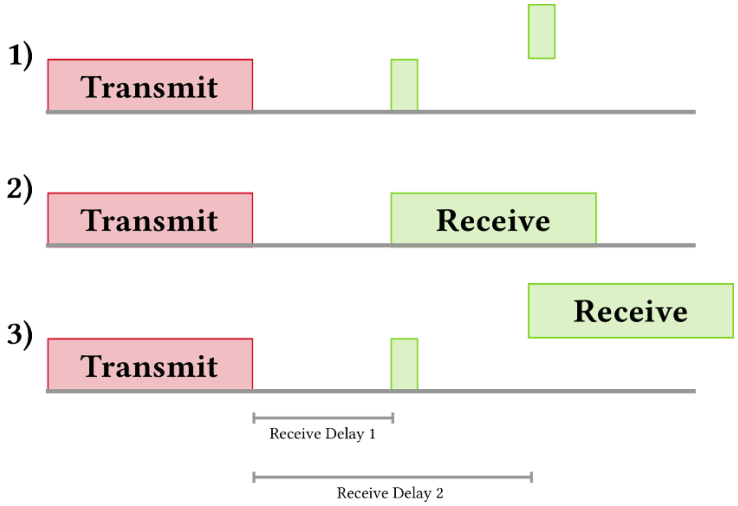

Fig. 2: Class A behaviour [28]

- **Class B:** In addition to the features included in class A devices, class B devices will open new receive windows at specified times. When working with these devices, GWs will transmit beacons to the end node in order to get synchronized and so the network knows when a device will be listening for downlink traffic. As easily deduced, class B devices will consume more power than class A devices since the first group will be in active mode more often to open those additional receive slots that characterize this class.
- **Class C:** The extra feature this class incorporates to class A characteristics is a continuous listening state for downlink traffic. This will cause an increment in the power consumption since these devices will be most of the time in active mode, whether it is for uplink transmission or for downlink traffic expectancy.

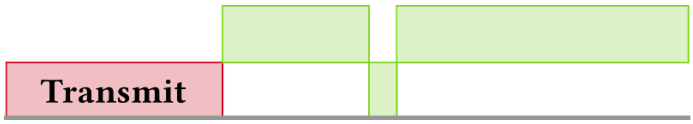

Fig. 3: Class C behaviour [28]

1.2 LoRa modulation

As introduced previously, LoRa modulation is a proprietary spread spectrum based on CSS modulation, which means it can work well with channel noise, multipath fading and the Doppler effect. It was patented by Semtech in 2014 [24]. It includes Forward Error Correction (FEC) and uses chirps, linear frequency modulated pulses, to encode the information to be transmitted [22].

There are two types of chirps, those called up-chirps, and those called down chirps, having all of them practically the same duration. During this interval of time, the chirp changes from an instantaneous frequency value f_0 to another, f_1.

Up-chirps start with a frequency value $f_0 = f_{min} = +\frac{BW}{2}$ and end with $f_1 = f_{max} = -\frac{BW}{2}$. With down-chirps it happens otherwise i.e., from $f_0 = f_{max} = -\frac{BW}{2}$ to $f_1 = f_{min} = +\frac{BW}{2}$. Both up-chirps and down-chirps have constant amplitude [24].

LoRa modulates these pulses, encoding the data to be transmitted into the chirps. In this case, and as stated in [18], "the trade-off is between the larger time/frequency occupation with respect to improved robustness against interferences".

1.3 Spreading Factor

The Spreading Factor (SF) is defined in [23] as "the ratio of rate of generation of chips where each bit of information is encoded as SF chips and 2^{SF} chips make one symbol".

It can take six different values: 7, 8, 9, 10, 11 or 12. With higher SF value, we obtain greater robustness against interferences, but also longer airtime, as well as higher values of signal-to-noise ratio (SNR), sensitivity and range. It's also of great interest to know that all of these SF values are orthogonal between each other. This means, two or more messages overlapping on time can still be correctly decoded if they used different SF values. Regarding this characteristic, in [18] the authors claim that, if the power of the interfering signal happens to be greater than the power of the desired signal, both signals cannot be received simultaneously.

Observing the formula that describes the bit-rate (R_b), it is possible to deduce that a longer airtime will be derived from a higher SF value. The bit-rate is defined as:

$$R_b = SF \cdot \frac{BW}{2^{SF}} \cdot CR \ [bits/s] \quad (1)$$

Where SF is the Spreading Factor, BW is the Bandwidth and CR is the Coding Rate.

1.4 Carrier Frequency

The Carrier Frequency (CF) refers to the centre frequency used for LoRa transmissions. LoRa uses frequencies on the ISM bands, which for Europe are the bands 868MHz and 433MHz. Therefore, as stated in The Things Network (TTN), Germany (or any European country) would use the frequency plans EU863-870 and EU433, as one can find in the LoRaWAN regional parameters document [25].

For EU863-870, there are several sub-bands predefined for uplink as well as for downlink transmissions [26]:

- Uplink:
    1. **868.1:** Bandwidth 125, SF 7-12.
    2. **868.3:** Bandwidth 125, SF 7-12 and Bandwidth 2500, SF 7.
    3. **868.5:** Bandwidth 125, SF 7-12.
    4. **867.1:** Bandwidth 125, SF 7-12.
    5. **867.3:** Bandwidth 125, SF 7-12.
    6. **867.5:** Bandwidth 125, SF 7-12.
    7. **867.7:** Bandwidth 125, SF 7-12.
    8. **867.9:** Bandwidth 125, SF 7-12.
    9. **868.8:** Frequency Shifting Keying (FSK)
- Downlink:
    1. Uplink channels 1-9 (RX1)
    2. **869.525:** Bandwidth 125, SF 9 (RX2)

1.5 Transmission Power

LoRa's working power ranges from -4dBm to 20dBm, but depending on the LoRa device the Transmission Power is limited to 2dBm to 20dBm, where power values higher than 17dBm can be used only on a 1% duty cycle, due to hardware limitations.

1.6 Bandwidth

Bandwidth (BW) refers to the width of the frequency band used in the LoRa transmission. There are three possible bandwidth configurations to use in LoRa: 125 kHz, 250kHz and 500 kHz. When choosing a higher bandwidth value, the sensitivity of the channel decreases but the capacity is increased [23]. The usual BW used is 125kHz.

1.7 Coding Rate

The Coding Rate (CR) resembles the FEC rate of LoRa. The CR is calculated as $CR = N/M$ where M goes from 5 to 8, and corresponds to the codeword length, and N is always 4, which is the data block length [18]. Therefore, it can only take the values: 4/5, 4/6, 4/7, 4/8.

The Coding Rate is used as protection against bursts of interference, presenting more protection with higher values of CR, but increasing airtime.[1]

1.8 LoRa Packet Format

The packet structure may include 4 parts, of which the header and a 16-bit CRC are optional, and the preamble and the payload must be present. [1]

The preamble is programmable from 6 to 65.532 symbols and has four fixed symbols at the end, making its maximum length extensible up to 65.536 symbols. This preamble is used for synchronization purposes, between the receiver and the transmitter. [24]

Previously, we talked about up-chirps and down-chirps, related to the fact that LoRa is based on CSS. Following this line, the preamble of the LoRa packet contains a programmable sequence of these chirps that facilitate the detection of the start of a frame. Then, two more chirp symbols follow this sequence, used to encode the sync word; and two other downchirp symbols end the preamble, used to synchronize on frequency. To differentiate devices from two different networks, the sync word can be of use if different sync words are used for each network.

As the authors explain in [24], the usual procedure is that the sync-word-chirps modulate opposite values, so once three consecutive chirps have been detected, let's say the first one was unmodulated and the two following are modulated with opposite values, then the new frame is detected. After the preamble, a quarter of a symbol time is included so the receiver can adjust in time.

In Fig. 4 we can observe the structure of the preamble just explained whereas in Fig. 5 we find the Spectrum capture of a LoRa packet. As it can be seen on the Figure, it starts with the mentioned sequence of up-chirps and down-chirps, until it reaches a point where two opposite values occur, leading to the frame itself, with an uneven representation.

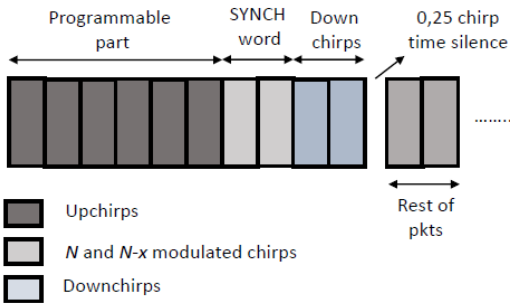

Fig. 4: Preamble structure [24]

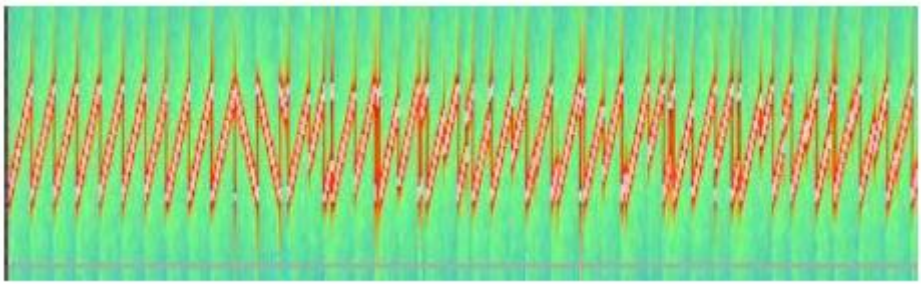

Fig. 5: Spectrum capture of a LoRa packet [24]

The preamble could be followed by an optional physical header which contains the header Cyclic Redundancy Check (CRC), present only in uplink messages; the FEC rate of the payload and the payload length, in bytes. In case all three of these parameters are known beforehand, the header can be omitted which would lead to a decrease into the airtime of the packet. If this last scenario applies, these parameters have to be fixed beforehand at the receiver as well as at the transmitter side, which is called *implicit header mechanism*.

After the physical header, we find the Payload, which may contain LoRaWAN layer control packets or data packets themselves. The LoRa packet structure can be seen in Fig. 6.

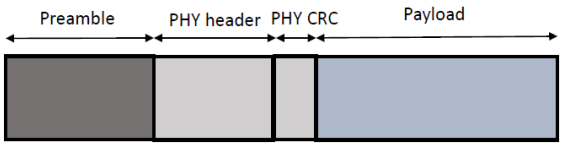

Fig. 6: LoRa packet format [24]

1.9 Time on Air

In LoRa, the Time on Air (ToA) corresponds to the transmission delay. Different other delays exist in LoRa, related to software or propagation, but its values take very low values and therefore, they're neglected.

In [18], the authors state that the ToA can be divided in a fixed part, composed by the preamble, the start of frame delimiter (SFD) and the physical header; and a variable part that depends directly on the payload.

Finding information about the equation followed by the fixed part is not so accessible, but in this same paper, the authors rely on the equation included in the SX1272 transceiver datasheet, found in equation (2).

$$T_{fixed} = [20.25 + \left(\frac{28 - 4SF}{SF - 2O}\right)\frac{M}{N}]T_C \quad (2)$$

where SF corresponds to the Spreading Factor, M to the codeword length and N to the data block length. This last term, M/N can be substituted for the value of the CR, as it is defined in the same way. *O* is an additional overhead included in case the SF takes the values 11 or 12, when its value will be 1. Otherwise, it will be 0, cancelling the term 2*O*. T_C is the chirp duration, defined as mentioned before, as $2^{SF}/BW$.

About the variable part, according to the authors in [18] it follows the formula contained in (3):

$$T_{variable} = [\left(\frac{8L - 16}{SF - 2O}\right)\frac{M}{N}]T_C \quad (3)$$

Where L is the payload length in Bytes and 16 is the CRC length in bits, if present. Unfortunately, it is not easy to find any other documentation where the calculation of the ToA is included, giving explicit formulas. Most of the papers mentioning it, directly refer to the airtime calculator provided by Semtech, which is no longer available. Anyhow, there exist another online calculator provided by TTN, which can be found in [30].

The total transmission delay (D_{TX}) is the addition of these two parts composing the ToA:

$$D_{TX} = \left[20.25 + \left(\frac{28 - 4SF}{SF - 2O}\right)\frac{M}{N}\right]T_C + [\left(\frac{8L - 16}{SF - 2O}\right)\frac{M}{N}]T_C \quad (4)$$

1.10 Adaptative Date Rate (ADR)

As defined in [31], "Adaptive Data Rate (ADR) is a mechanism for optimizing data rates, airtime and energy consumption in the network", built into LoRaWAN.

It usually works on devices with sufficient stable RF conditions (it often means the devices are static), which leads to the device itself being the one deciding whether ADR should be used. If the device wants to use this mechanism, it will send the ADR uplink bit included in its uplink packets [24], allowing the network server to manage its parameters in order to comply with the aim of the ADR. Anyhow, in case the device doesn't want the server to take part, it exists the possibility of using the ADR mechanism on the end device.

In order to determine the optimal data rate, the network uses some uplink messages to be used in measurements. As included in [31], currently the TTN makes use of the 20 most recent uplink messages counting only from the moment the ADR bit was set and discarding all measurements once this ADR bit is taken down. The measurements include signal-to-noise-ratio (SNR), number of gateways that received each uplink and frame counter.

The goal is to calculate the so called *margin*, which provides information about the extent the data rate can be increased. It is calculated as the difference between the measured SNR of the best gateway and the required SNR needed to demodulate a message for the corresponding data rate used.

According to [31], there exist four moments during the communication when an ADR is sent or scheduled. The first moment corresponds to the initial ADR request, although it is only used for US915 and AU915, therefore not considered in this document. The second makes reference to a regular ADR request, meaning that this request is planned for the instant when enough messages to carry out the before mentioned measures exist, and the data rate is not optimal. Although it is

important to highlight that this request is only scheduled, not sent, and will be attached to a downlink message (for example, to an ACK). The third case is an ADR request, sent when the previous conditions apply and the device uses DR0, which means SF12 and BW125 for most regions. The last one is an ADR request sent when the ADRAckReq bit is set, which usually (although the number might change depending on the device) after 64 uplink messages with no downlink message happens by default.

If several ADR requests are rejected, these will be scheduled no more. This same process is also explained in [24], introducing the following parameters to later represent the flow graph of the ADR's behaviour:

- ADR_ACK_LIMIT: set to 64.
- ADR_ACK_DELAY: set to 32.
- ADR_ACK_CNT: increased in one for every uplink message sent.
- ADRAckReq: active when ADR_ACK_CNT is higher than ADR_ACK_LIMIT.

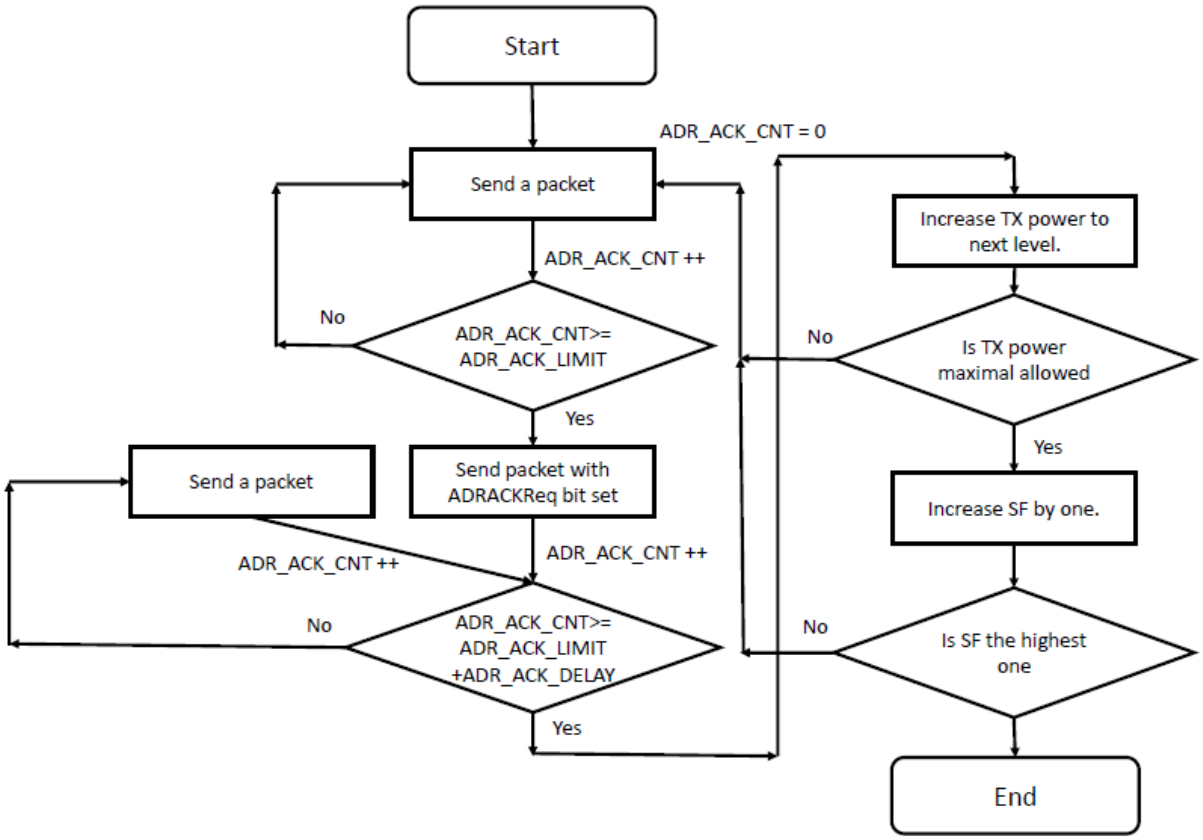

Fig. 7: ADR's functioning flow graph [24]

1.11 Limitations

For the TTN, there exists a Fair Access Policy that determines the limit amount of data end-devices making use of it can send. The maximum uplink airtime is limited to 30 seconds per day, so every 24 hours, per node. Furthermore, the maximum number of downlink messages per day is set to 10, per node. If a private network is used, then these limitations don't apply.

Additionally, governments set a maximum duty cycle for radio devices, which is usually limited to 1%. In [32], these limits on duty cycle are specifically mentioned for the different sub-bands used in Europe. These are:

- 863.0 – 868.0 MHz: 1%
- 868.0 – 868.6 MHz: 1%
- 868.7 – 869.2 MHz: 0.1%
- 869.4 – 869.65 MHz: 10%
- 869.7 – 870.0 MHz: 1%

We will find later how these limitations affect the different deployments making use of LoRa, and if they result in a great disadvantage or not.

Chapter 2: Literature review

2.1 Motivation

LoRa and how it works is a topic highly present for IoT developers, although not as many answers as desired are easily found. Even so, the number of paper-works using LoRa is surprisingly high, although these papers usually do not focus on how LoRa behaves in the specific deployment they present but find some other focus. In any case, they still result of great usefulness since they provide an overview of on what kind of applications LoRa is being used, as well as what values its configuration parameters take. Thanks to that, it is possible to adapt the experiments aiming to test LoRa, to real-life values already used in some deployments. Since this study is willing to test how LoRa behaves under different circumstances, these resources are to be considered.

Following this goal, this chapter includes a review of some LoRa applications with different aims, deployments, and conclusions, willing to give a wider overview on LoRa in the so-called real world. First, a table containing the different parameters used in the experiments to be reviewed will be included, highlighting those parameters that might be most interesting for the future research including, among others, number of nodes used, SF, BW or range. Then, some of the papers present in the table, will be deeper explained, especially those focusing on LoRa's functioning.

2.2 Classification

Table 1 shows a collection of LoRa-based IoT applications, used in this study to set an example of what values are being used in real-life configurations of LoRa deployments for its different parameters. It also shows two of the KPIs that will be evaluated later in our experimental phase: ToA and range. In the table only specifically mentioned values are included, together with some brief clarifications if needed for the complete understanding of the table.

The last column shows the experimental approach. When real deployments have been used, then it will be labelled as experimental. If the authors of the referred paper worked with a simulation, it will be indicated as so.

In the next sub-chapters, some of these works will be deeper explained, given that they focus on the behaviour of LoRa and therefore are of great interest to, together with the results we will show in Chapter 3**: Experimental setup**, get a wider overview of the functioning of LoRa under different circumstances and related to different testing goals.

Everything included in the table is explained in its corresponding paper, so for a complete understanding it is also important to read the papers of the different applications, relying to the original paper in case of mismatches.

Table 1: Compilation of LoRa-based IoT scenarios

Application name	Sending interval	Payload (bytes)	Nodes	SF	ToA	Range	Type of approach
LoRaSIM [1]	22 min	20	2	7-12	7.07 ms - 1.71213 s	2.6 km (rural) 100 m (urban)	simulation
Mobile LoRaWAN [2]	5 s (not reached)	50	2	12	1.365 s	30km	experimental
Single Node Throughput [3]	-	1, 25,51	1	7-12	-	2.8km	simulation
LoRa Indoor Deployment [4]	10 s 2 min 30s	-	9	12	-	50cm-60m	experimental
LoRa Indoor Propagation [5]	-	-	1	12	-	Concrete building, no size specified	experimental
LoRa FABIAN [6]	-	25	-	7-12	-	3km-6km	experimental
LoRa Wi-Fi [7]	-	-	1	-	-	6 km 20 km	experimental
LoRaWAN Channel Access [8]	-	51	-	7-12	-	-	Mathematical model
PHY and Data link testbed [3]	-	-	-	7-12		2.8km	experimental
LoRaWAN Nordic Cities [9]	6 min	54	10	-	-	-	experimental
uPnP_WAN [10]	-	-	-	12	-	3.5km	experimental
Throughs Water Level monitoring system [11]	30-600 s	26	5-100	-	-	0.5 - 2.7 km	experimental.
EM Energy Harvester [12]	-	8	-	12	-	-	experimental
WaterGrid-Sense [13]	-	18	15	7-12	-	1.25 km	experimental
Smart Irrigation System [15]	-	-	1	12	-	7 km	experimental
Smart Building [16]	1s	-	71	-	-	12 floor building	experimental
Wellbeing monitoring [17]	5s	-	1	12 (125kHz)	-	570 m	experimental
Smart Aquaculture [19]	0.5s, 1s, 5s	44, 56, 80, 128	1	-	-	200 m, 400 m	experimental
Sailing monitoring [20]	2s	96	-	7	-	400 m, 1 km	experimental

2.3 LoRaSIM

In [1], the authors studied the scalability of a LoRa network working over LoRaWAN for a build-up environment, an urban scenario. They divided the experiment in three parts: (a) LoRa Link Behaviour, (b) LoRa Simulator and (c) LoRa Scalability Evaluation.

In part (a), they established models by means of practical experiments to describe the dependence of the communication range in the communication settings SF and BW; and the capture effect of LoRa transmissions depending on transmission timings and power. For this, they used the XRange SX1272 LoRa module from NetBlocks. They introduce a mathematical model that will be more extensively considered in the next chapter. The final outcome of this first part is a model of collision used in the next section of their work.

In (b), the authors use a simulator to analyse the scalability of LoRa networks. This part is developed by means of a simulation tool, LoRaSIM, "a custom-build discrete event simulator implement with Simply" [1]. Even so, to make sure their approach has a practical relevance, they use the previous experiments as base to calibrate the simulation since, as they argue, it wouldn't be viable to evaluate the scalability of large-scale LoRa deployments due to the expenses this kind of experiment would generate and an experimental deployment would limit the number of possibilities regarding configurations and topologies, which results of great interest for the study. The authors propose three different scenarios, each one of them with an experimental set of parameters. The first set, single sink (N nodes transmit to one sink M) contained the parameters included in the following table:

Table 2: Parameter setting for Experiment Set 1. [1]

Parameter	**SN_1**	**SN_2**	**SN_3**
TP (dBm)	14	14	14
CF (MHz)	868	868	868
SF	12	6	12
BW (kHz)	125	500	125
CR	4/8	4/5	4/5
λ (ms)	$1x10^{-6}$	$1x10^{-6}$	$1x10^{-6}$
B (byte)	20	20	20

Where TP is Transmission Power, CF carrier frequency, SF Spreading Factor, BW bandwidth, CR Code Rate, λ average packet transmission rate and B, packet payload.

The authors selected two parameters to evaluate the outcome of the different configurations: Data Extraction Rate (DER) and Network Energy Consumption (NEC). DER is defined as the ratio between received messages and transmitted messages over a period of time, while NEC is defined as the energy spent to extract a message. This last parameter depends on depends on the number of nodes, frequency of transmissions and transmitter communication parameters.

The initial sending interval stablished is 16.7 min and the payload is of 20 bytes (see Table 1 and 2). For the first configuration, robustness was sought leading to the longest airtime(1712.13ms). The second configuration aimed to have the shortest airtime (7.07ms), and the third included commonly used parameters. After a running simulation of around 58 days, the authors met the following conclusions:

- With an increasing number of nodes, the Data Extraction Rate (DER) drops exponentially in all cases.
- The difference in DER is significant when comparing the configuration with the longest and shortest airtime.
- The default LoRaWAN configuration (SN_3) is very close to the configuration with the longest airtime.

Following the results with the third configuration, the authors calculated it could support N=120 nodes for a DER>0.9, with a range of 100m in a built-up environment, finally concluding that "many applications (such as building automation) could not be supported by a LoRa system. Furthermore, to comply with European regulations, the sending interval should be of 22 min instead of 16.7 min so they maximum duty cycle would not be exceeded.

For the second experiment set, an evaluation of the impact of dynamic communication parameter selection on DER and NEC is carried out. The authors find a huge improvement compared to the first experiment set, reaching up to N=1600 nodes with DER>0.9 and minimised airtime, also achieving a huge improvement on NEC. The configurations used randomly placed nodes around the sink. Even so, it is important to highlight that, as they claimed, "this achievement is not practical and relies on quite optimistic assumptions", not quite an existing scenario in real deployments.

On the third and last experiment set, the authors test the impact of the number of sinks, using the SN_1 configuration. For each experimental run, they use an increasing number of sinks M. They find that with higher number of sinks, a significantly DER increase occurs. Moreover, contrary to what they expected, the network doesn't get saturated which they attributed to the fact that "with an infinite number of sinks, each node might find such a sink avoiding packet loss".

The last conclusions met are the following:

- Regarding scalability, using a typical LoRaWAN setup, the number of nodes supported does not represent a sufficient number for applications related to, for example, smart city deployments.
- Dynamic LoRa settings have a huge impact on network scalability, being however not yet achievable since specifications for gain protocols and mechanism dynamics are yet to be given.
- The capture effect has a significant impact on achievable DER.
- Multiple sinks improve the DER.

2.4 Mobile LoRaWAN

In [2], authors aimed to evaluate the Range of LoRa technology. Real-life measurements were carried out at the city of Oulu, Finland, during 14 days in spring/summer season, under different weather conditions. The city counts with around 200 000 habitants, it's mainly plain and the highest buildings existing in that moment are 12 floors high. Given that the city is located at the coast, some measurements were carried out on the water.

For all measures, the position of the base station was fixed, with an end device on a moving car for or boat, which sent a packet periodically containing a sequence number and GPS coordinates, used to estimate the packet loss rate and the position of a node.

A Kerlink's LoRa IoT station, connected to the biconical D100-100 antenna from Aerial, located at the University of Oulu antenna tower, 24 m over the sea-level, was used as base station.

As end devices, authors used LoRaMote, with a Semtech SX1272 transceiver with Planar-F type printed circuit board antenna, with firmware version 3.1. Each node included also a GPS receiver and a set of sensors. SF12 was used, together with BW 125kHz.

The sending interval was set to 5 seconds which obviously, and as the authors say, was not an achievable target due to the existing restrictions. All nodes were working under a TP of 14dBm.

Authors divided the evaluation distances in 5 groups between on land and on water measures, obtaining the results included in the following tables:

Table 3: Results of measurements with car [2]

Range	Number of transmitted packets	Number of received packets	Packet loss ratio
0-2km	894	788	12%
2-5km	1215	1030	15%
5-10km	3898	2625	33%
10-15km	932	238	74%
Total	6813	4506	34%

Table 4:Results of measurements with boat [2]

Range	Number of transmitted packets	Number of received packets	Packet loss ratio
5-15km	2998	2076	31%
15-30km	690	430	38%
Total	3688	2506	32%

The first point the authors highlight is that, given the total number of measurements carried out (around 10 000), "this is not enough to get the results which will be statistically meaningful" [2]. They attributed this low number of measurements to the restrictions already mentioned, but in any case, it is a good start to provide an insight into LoRa's capabilities.

2.5 Single Node Throughput

In paper [3], an experiment to evaluate the maximal throughput a single node can obtain was carried out. When written this paper, the authors stated different purposes, mainly related to LoRaWAN. Given so, we will focus on the part concerning LoRa, which corresponds to the single node throughput experiment.

This experiment, aiming to evaluate the maximal throughput that a single device can obtain, was set with the following characteristics:

- Sending interval: the minimum allowed by the channel limitations and the protocol (not specified)
- 6 channels
- BW=125kHz
- SF: From 7 to 12

- MAC header size: 13 bytes

The results obtained, depending on the payload size, are included in Fig. 8. It was found that the maximum payload size allowed by this implementation was of 51 bytes.

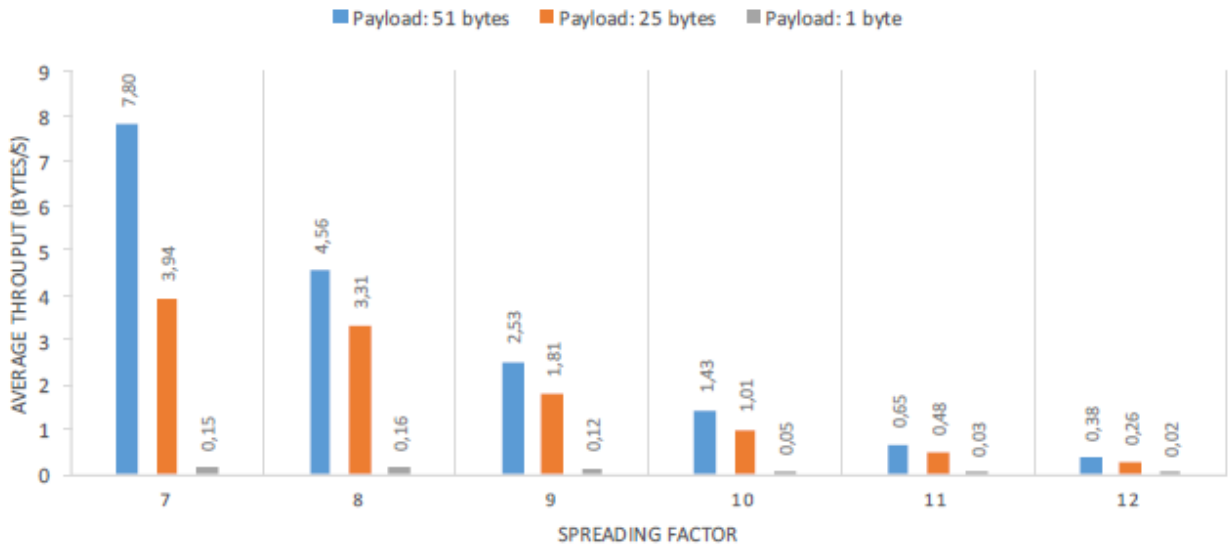

Fig. 8: Maximum throughput attained by a single device using LoRaWAN [3]

The authors found that at low packet sizes, the limiting factor was the duration of the receive windows, instead of the channel duty cycle limitations, as possibly expected. The *problem* is that "the device has to wait for the two downlink receive windows following the transmission to be over before sending another packet." [3].

They also remark that the maximum size of the frame depends on the data rate used, and that LoRaWAN lacks a mechanism to split large payloads over multiple frames. They propose a what they call conservative approach: to never try to send more than the smallest maximum payload size, which is 36 bytes. Anyhow, this would lead to a loss of capacity for large amounts of data. To solve this, the authors propose adding a fragmentation mechanism in LoRaWAN.

Besides that, two experiments are conducted, The first one focusing on checking the decoding performance of LoRa receivers. Following this aim, 10 000 packets were sent from a LoRa device to the GW, and the Received Signal Strength Indicators (RSSI) of the received packets were recorded while moving the end-node. The GW was placed indoors while the end-device was outdoors in a built-up environment. The BW used was 125kHz, and CR 4/5. It was found that at around 100m, packets started to get lost. The minimal RSSIs can be observed in Fig. 9:

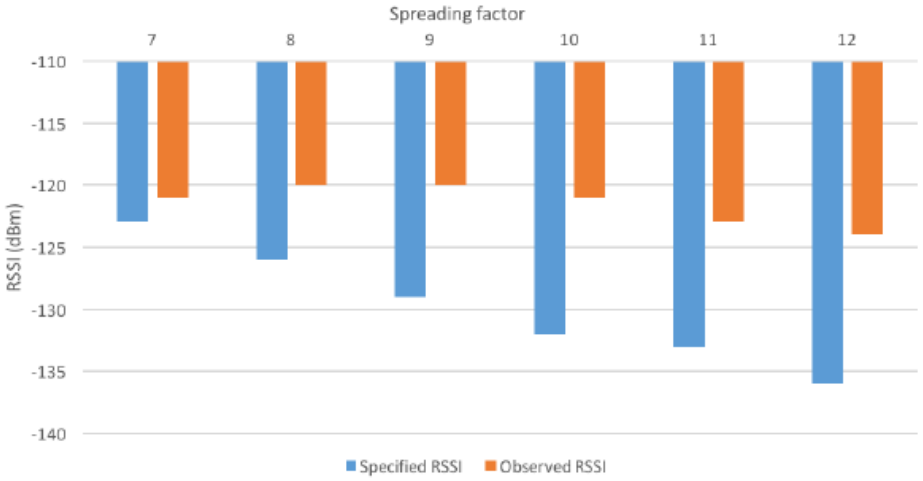

Fig. 9: Minimal observed RSSIs with different spreading factors [3]

The author observes that the results obtained are slightly above the specified values and that the decrease expected with the increase of the SF doesn't occur.

The second experiment intents to test the network coverage of LoRa. The experiment took place in a suburb of Paris, with low-height buildings. The temperature was 15ºC, and the humidity was of 55%. The GW was placed on a window (outside) of the second floor of a house (around 5m of elevation), and the end-node was located on top of a car. The different testing sites were placed at 650m (A), 1400m (B), 2300m (C),2800m (D) and 3400m (E) away from the GW. In Fig. 10, the packet delivery ratio of different SF with various distances is shown. The results showed that for a SF 12, more than 80% of packets were received at a distance of 2800 m, whereas when using SF 7 no packet was received.

In any case, the authors note that what was configured to perform the test, does not adjust to what happens in reality since the SF value increases automatically if a lower value fails. Therefore, in a network with LoRaWAN, a higher delivery ratio can be achieved.

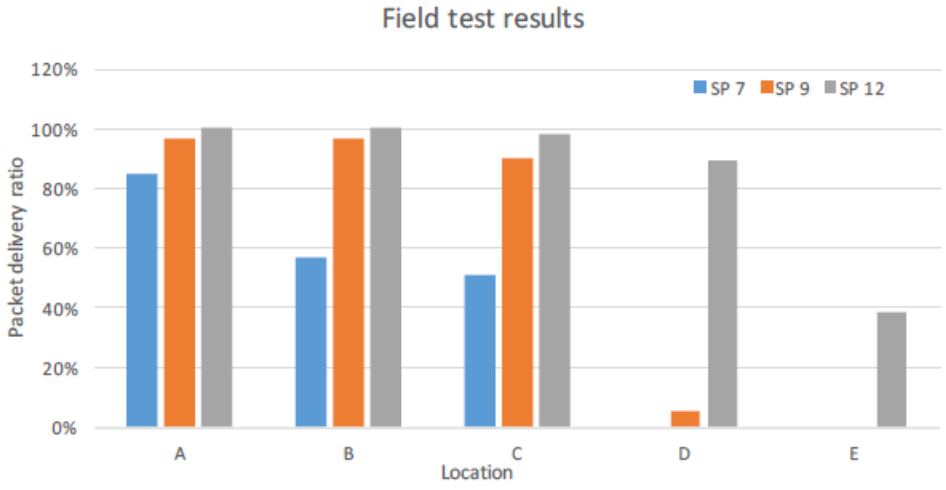

Fig. 10: Packet delivery ratio of the LoRa field test [3]

2.6 LoRa Indoor propagation

Since smart buildings are one of the applications that arise more interest, what is presented in [5] might be of great help. In this paper, the authors develop a measurement of an indoor propagation

of LoRa signal in a reinforced concrete building in Prague, Czech Republic. The measurements are divided in two cases, with a mobile end-node and a fixed receiver in the middle of the building. In the first case, the receiver is located in the basement of whereas in the other case, it is located on the roof. The final finding is that the best signal coverage corresponds to the second location of the receiver, i.e., on the roof.

The devices used are, as the transmitter an IMST iU880A and as the receiver, a iC880A with the SX1301 chip. For each measurement, the location of the end-node changes. The locations of the transmitter can be observed in Fig. 11 and Fig. 12. From each location, 10 messages are sent, representing each placement one payload size.

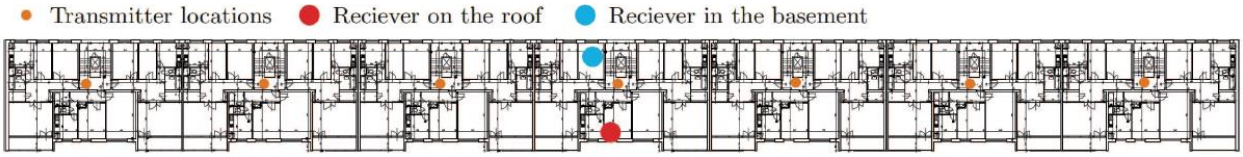

Fig. 11: Longitudinal section through the building with labeled transmitter and receiver locations [5]

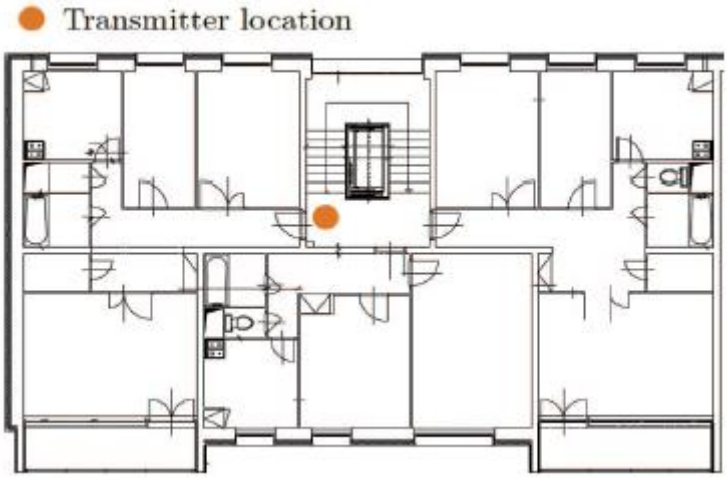

Fig. 12: Floor-level detail of one entrance with a labeled transmitter location

The output power of the transmitter is set to 20dBm, data rate to 0, SF 12, BW 125kHzand bit rate 250 bps. The results of the measurements are shown in terms of the Table included in Fig. 13. In Fig. 14, the results of the second case (receiver on the roof) are shown, and in Fig. 15, those for the first case (receiver on the basement).

the average (S) proportion of a reference number [%]	
0 – 4	
5 – 9	
10 – 14	
15 – 19	
20 – 24	
25 – 29	
30 – 34	
35 – 100	

Fig. 13: Values for visualization [5]

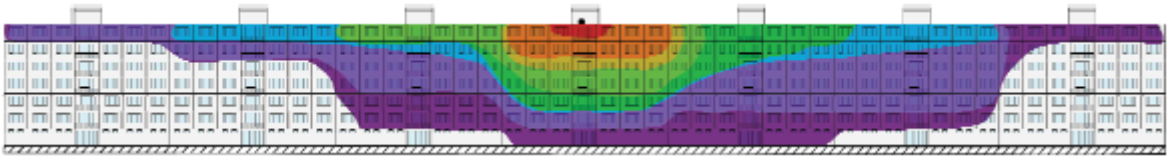

Fig. 14: Visualization of the results with the receiver located on the roof [5]

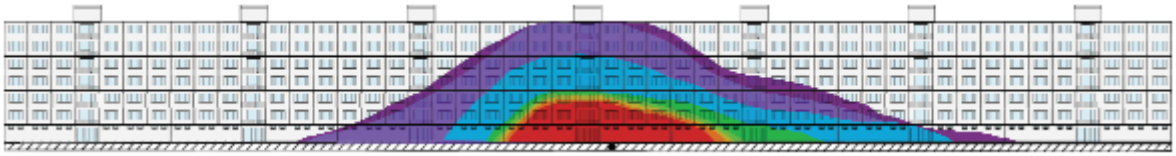

Fig. 15: Visualization of the results with the receiver located in the basement [5]

The conclusion reached claims that the LoRa signal spreads easier and wider when the receiver is located in a position above the end-node, in this case, on the roof. Nevertheless, a LoRa device with such setting is not able to cover the entirety of the building, where the best coverage occurs in the entrance where the receiver is located, while packet loss increases rapidly in other entrances of the building.

2.7 LoRaWAN channel access

The goal of the authors in [8] is to survey LoRaWAN operation, focusing on performance evaluation of its channel access, to evaluate its capability of supporting massive machine type communication, over Class A devices.

The scenario used consists of *N* end-nodes connected to a GW, operating in 3 main channels and one downlink channel, with BW 125kHz, with SF 7-12, and 51 bytes of payload (biggest payload at the lowest data rate). In Fig. 16 the results are shown in terms of Path Loss Ratio (PLR), with different values of *N*. The results highlighted show that, for a load less than 0.1 packet/s, PLR is negligible, which for *N*=100 end-devices, each of them could generate a packet less than once per 20 minutes; or for *N*=5000, they could generate per day less than 2 packets. When the load is increased, PLR and PER (Packet Error Rate) significantly increase. They conclude that this reality limits the possibility to use LoRaWAN technology in many scenarios of smart city.

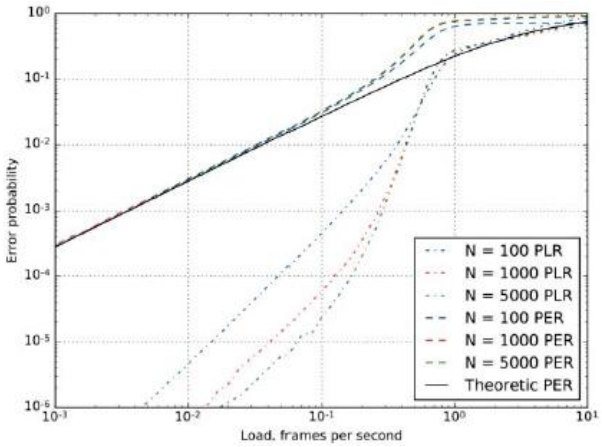

Fig. 16: PER and PLR vs. Network load [8]

Chapter 3: Experimental setup

This chapter shows our own experimental setup. From Chapter 2**: Literature review**, it was possible to identify the most important KPIs used to evaluate the performance of LoRa, together with the parameters that affect them. These, presented in Table 5, will be used on the development of this experimental part.

Table 5*:* KPIs and parameters to be considered in the experimental phase.

KPIs	Parameters
Packet-loss ratio	Range
Delay	Spreading Factor
Power consumption	Payload
	Class

The tests were carried out in the city of Bremen, Germany. Its dense urbanized zones are limited to the city centre, being most of the city characterized by big green spaces and residential houses of mainly 2 floors.

During the whole experimental phase, we used a Lopy4 connected to an expansion board 3.0 together with the LoRa (868MHz/915MHz) & Sigfox Antenna Kit, all of it of Pycom.

To test the different KPIs, different changes in the parameters proposed had to be introduced, leading to the proposal of 3 different scenarios. The first one, a static setup and the other two, mobile setups but with different configurations.

All of these experiments were done through the TTN, where the application and device were registered. An HTTP Integration was configured so all the metadata of the different transmissions could be logged into a Google spreadsheet. The code used is a slightly modified version of the code available on the Pycom libraries, specifically that called *lorawan regional examples*, for Europe. In the following sub-sections all three scenarios will be explained, and the results will be shown.

3.1 Scenario 1: static setup

For this first scenario, the node was located into an apartment on the third floor of a 4-floors building. In Fig. 17 the position of the node is represented, together with the two GWs in range from its position.

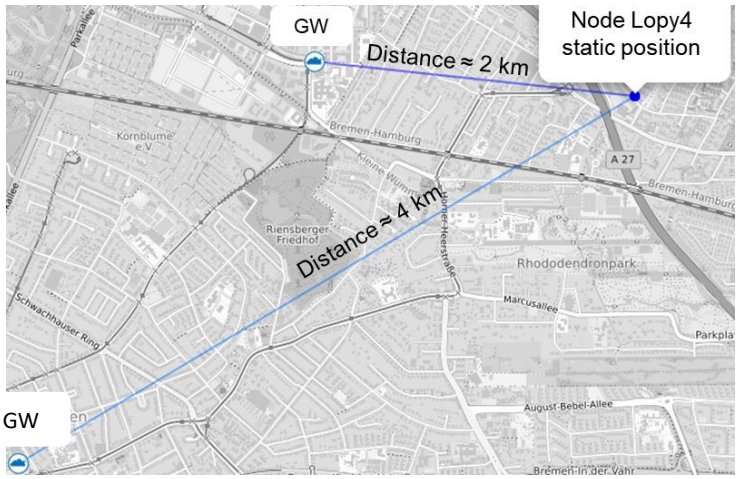

Fig. 17: Position of the node and the GWs in range

The GW 2 km away from the node, is in an industrial zone, next to the University of Bremen. This area is not densely built-up, with buildings up to 5 floors. The line joining these two points, GW-node, becomes denser the closer to the node, although, again, the highest buildings do not reach more than 5 floors.

The 2nd GW, 4 km away from the node, is next to the city centre, in a dense urban zone where the buildings are not lower than 3 floors. In this case, when following the line between GW and node, the density of buildings doesn't significatively change, although the height tends to be lower.

In this first scenario, three KPIs were measured: delay, packet-loss ratio and power consumption. To measure each one of them, different configurations were used:

To test the delay (D_{TX}), the same value of SF was used while the payload changed. As all values of SF were tested, the procedure followed consisted in fixing the SF value while changing the payload, and repeat this 6 times, i.e., one per SF value.

The payload was configured to take values from 1 to 51 bytes, since 51 bytes is the maximum payload allowed on TTN for SF 10, 11 and 12. The sending interval was set to 30 s aiming to imitate the sending interval used in some applications found in the literature review. Again, it was tested for all SF values. The experimental results were extracted from the TTN console, as part of the metadata thrown for each packet received. These results were compared with the expected transmission delay, also called airtime, calculated as:

$$D_{TX} = \left[20.25 + \left(\frac{28 - 4SF}{SF - 2O}\right) \cdot CR\right] \cdot \frac{2^{SF}}{BW} + \left[\left(\frac{8L}{SF - 2O}\right) \cdot CR\right] \cdot \frac{2^{SF}}{BW} \quad (5)$$

Where SF is the Spreading Factor value, CR the coding rate (in our case, 4/5), L is the payload size in bytes, BW is the Bandwidth (125 kHz) and *O* is an additional overhead for SF 11 and 12. For these values, *O* is equal to 1, and otherwise, to 0. This equation, found in (4), was adapted to our specific case.

The results can be seen in Fig. 18. The straight lines represent the experimental results whereas the dashed lines represent the expected results. The representation of the experimental results has a staired-shape because on TTN console, for three adjacent payload values, the airtime value given was exactly the same. Therefore, it appears to be constant for three values, and then it raises and follows the same path again.

As one can observe in the graph, with lower SF values, the difference between expected and experimental results don't differ in a great measure. Anyhow, this difference appears to increase as the SF value increases. Although it would be interesting to have an explanation for this phenomenon, unfortunately there is not much information available about how TTN actually works, which prevents us from further study at this point.

It is also possible to see how for higher SF values, the delay is considerably higher for the same payload size. This result coincides with what we expected, as this characteristic is part of the definition of the Spreading Factor: for higher SF values, the robustness offered is higher, but the airtime is also increased.

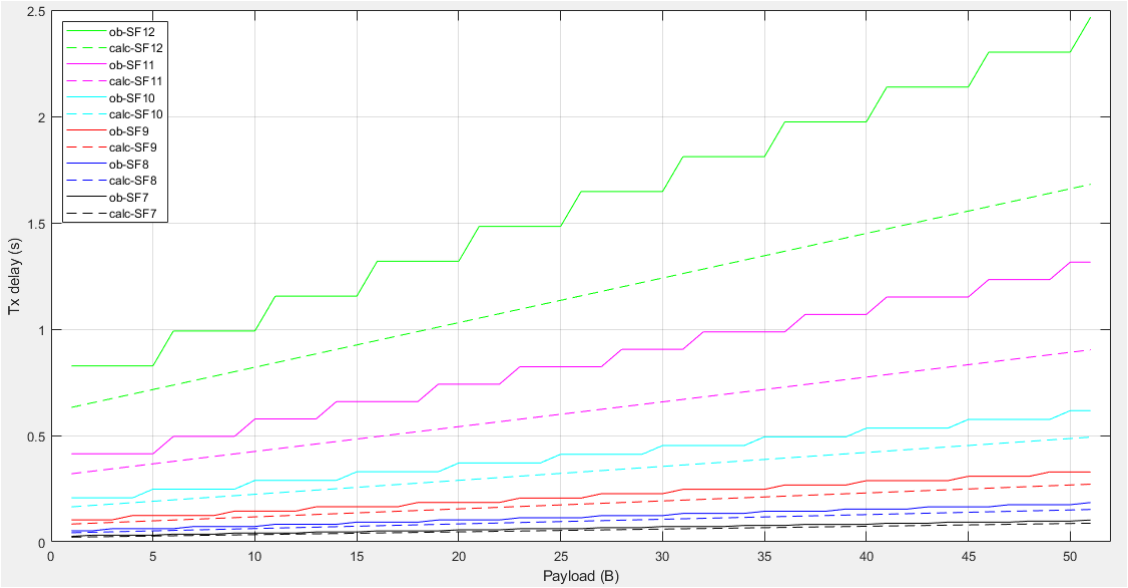

Fig. 18: Obtained transmisión delay vs. Expected transmisión delay

To test the packet-loss ratio (*PL*), we worked with a fixed payload of 50 bytes, again imitating one of the values found in the Literature review, used in a real-life application. This value was also chosen since it is very close to the limit value for SF 10, 11 and 12 (51 bytes), i.e, the worst case scenario.

The beginning of the transmission was bounded between 18:30 and 19:00 since a previous test-run was done for all SF values, starting at arbitrary time slots. Once all the results were obtained, they did not coincide with the expected, i.e., higher packet-loss ratio for lower SF values. Therefore, it was decided to do all the tests at the same time to check whether it influenced the results or not.

We also considered the existing limitations for LoRa, which are 1% of duty cycle and a maximum of 30 s of uplink transmission per day. The maximum number of packets (N_{max}) to be sent per day and the minimum sending interval (S) were calculated following the equations (6) and (7).

$$N_{max} = Floor(^{30}/_{ToA}) \quad (6)$$

$$S = \frac{ToA}{Duty\ Cycle} - ToA \quad (7)$$

The obtained minimum sending interval was rounded up to the next integer to avoid working with decimals. In Table 6 the values of N_{max} and S calculated for each of the SF values are shown.

Table 6: Parameters' values used for the tests

Payload (B)	SF	N_{max}	S (s)
50	7	307	10
50	8	171	18
50	9	91	33
50	10	48	62
50	11	22	131
50	12	13	228

It is interesting to highlight the huge difference between the values obtained for the different SF values. Choosing the most robust SF limits considerably the number of packets that can be sent per day, with a great increase in the minimum sending interval. These differences might be critical when choosing one or another SF value depending on the type of application to deploy.

For each SF value, the tests were run 3 times to be able to calculate the mean of the packet-loss ratio and the deviation of the results. This was done aiming to test how much the results obtained in different days would differ. The results are included in Table 7.

Table 7: Packet-loss ratio results for scenario 1

SF	P_{sent}	$\overline{P_{RX}}$	$\overline{PL}$	Deviation
7	307	253.67	17.37%	0.022879
8	171	159	7.02%	0.011696
9	91	85.67	5.86%	0.027655
10	48	46	4.17%	0.020833
11	22	21.34	3.03%	0.026243
12	13	13	0%	0

Information about the number of packets sent (P_{sent}), mean of the packets received ($\overline{P_{RX}}$), mean of the packet-loss ratio ($\overline{PL}$), and deviation is included.

This time, the packet-loss ratio resulted, as expected, higher for lower SF values, with an important difference between the two limit values. Surprisingly, no packet was lost in any of the tests for SF 12, which sets a very good precedent for future use. But, if we check more in detail, it's easy to spot the bigger difference existing between the results obtained for SF 7 with respect to those for SF 8, where the packet-loss ratio differs more than a 10%; whereas the difference between the other adjacent values is of, at most, 3%. This could be due to the fact that most developers and experiments of LoRa are done using SF 7, which would mean a lot more traffic for this SF than for the others, and therefore, a lot more of interferences, causing a higher packet-loss ratio.

Finally, the values obtained for the deviation are very low, which lets us claim that the results obtained can be trusted and can be used as an example for deployments with the same characteristics.

The last KPI to be evaluated in this scenario was the power consumption. The aim was to analyse how using Class A or Class C affected this KPI.

We chose analogic measurement in regards of the tools available on site. Anyway, and due to the covid circumstances, accessing to more sophisticated tools was not possible. Due to this, the multimeter used to measure the current was up to 2 decimals, so the measures taken are not as precise as we wanted to. The circuit used can be seen in Fig. 19. Even though, it is still possible to get a general idea of the power consumption depending on the class used.

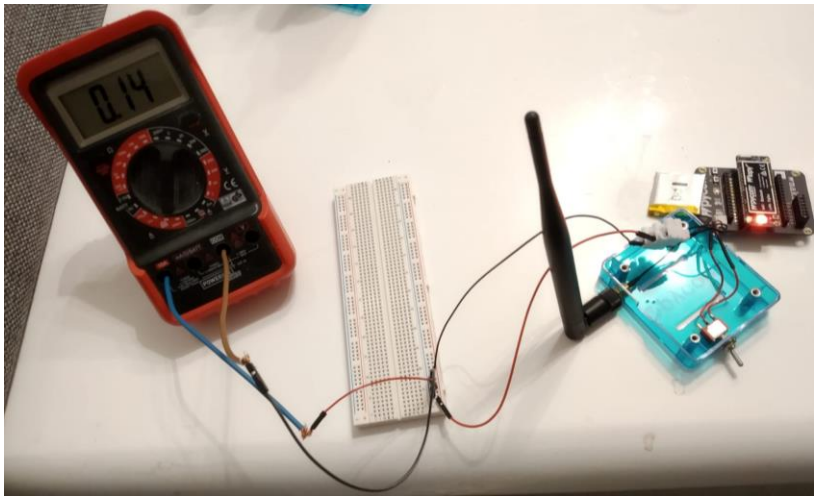

Fig. 19: circuit used to measure the current usage

For class A, when the Lopy4 was on stand-by state, the multimeter measured a current usage of 0.14 A and 0.15 A. Therefore, we can claim that the current used in this state oscillates from 140 mA to 159 mA. On the other hand, for class C while in this same state the current measured was comprised in between 160 mA and 169 mA. When a packet was sent, the current augmented in both cases on around 60-70 mA.

Together with the current measured and the voltage feeding the circuit (in our case, 3.77 V), it is possible to calculate the power (P) consumed using equation (8), where I is current and V, voltage. In the next chapter, the power consumption for all SF values will be represented.

$$P = I \cdot V \text{ [W]} \tag{8}$$

3.2 Scenario 2: mobile setup

The second scenario aimed to measure the packet-loss ratio and the maximum distance GW-node that could be reached in an urban environment, for example in Bremen. This time, the node was mobile, located inside a car, in the front seat, while the car drove through the city, getting closer and away from the GWs.

The payload chosen was of 1 byte, to maximize the number of packets to be sent. In this case, only SF 7 and 12 were tested, to represent the two limit values of LoRa. Again, the limitations imposed for LoRa were considered, and therefore we calculated the maximum number of packets that could

be sent per day. For SF 7, 1160 packets could be sent, while for SF 12 only 36 were possible to be used. Since using the minimum sending interval would limit the whole experiment time to around 50 minutes, it was decided to choose a higher sending interval, to extend the experiment time to 2:15 hours. For SF 7, the sending interval used was set to 10 s, and for SF 12, to 224 s. As done in the first scenario, both cases were measured three times to later obtain the mean of the results and the deviation.

Since the node would be moving and its position at each moment is of importance for the test done, the TTN Mapper [34] app available for Android was used for this purpose. This app throws as a result a map similar to that in Fig. 20.

The map shown corresponds to the city of Bremen, Germany. The coloured bullet points represent the different positions the node took during the test whenever a packet was received by any of the GWs in range. This means, if a packet was sent but not received, the position of the node at that moment is not included in this map.

The blue clouds are the different GWs found in range during the experiment. The bullet points are connected with straight lines of the same colour only to the GWs in range in the moment of the transmission of each one of the packets in the picture. This means, a bullet point will not have a joining line to all the GWs in the image, but only to those detected by it in that exact position. The colour of this line and the corresponding bullet point changes depending on the signal strength, and it follows the legend of the lower right corner of the picture.

The central part of the map coincides with the city centre, where a higher density of buildings is found, being around 6 to 9 floors high. As one gets away from the centre, in all directions, the density of buildings decreases and their height as well. On the outer rings of the city, so where the outer bullet points are found, the buildings are small houses of 2 floors, with a big separation between each other, and numerous green flat zones.

The path followed by the moving zone starts next to the upper GW in the picture. From there, it moved towards the city centre, so towards the central GW where the maximum number of bullet points is found. After that, we went to the airport in Bremen, on the lower left side of the picture, were only a few green and yellow bullet points can be found. Then again, we moved back to the city centre, from the left. From there, we drove towards the lower right part of the map to come back once again to the city centre to go to the upper right part of the map, where the transmission ended. This same path was followed the three times each SF was measured.

In the case of the SF 7, the maximum coverage registered is of 6569 m, also indicated on the picture. The mean packet-loss ratio obtained between the three measurements is of 57.47%, with a deviation of 0.125063.

In case of the SF 12, found on the Fig. 21, the maximum coverage distance GW-node recorded was of 6563 m, with a mean packet-loss ratio of 18.52% and a deviation of 0.042431.

In this scenario, the expectations of higher packet-loss ratio for lower SF values it's also met. In fact, the difference between the two limit values, under the same conditions, is astounding and greatly different to the results obtained for the static scenario. Anyway, considering the constant change of the environment, the place and the speed of the moving node, one could say that these results are pretty acceptable if it's not critical that all the data sent arrives to its destination in the application to be deployed under these circumstances. Also, the deviation values are low enough

to assume these values can set a precedent for future experiments working with the same conditions.

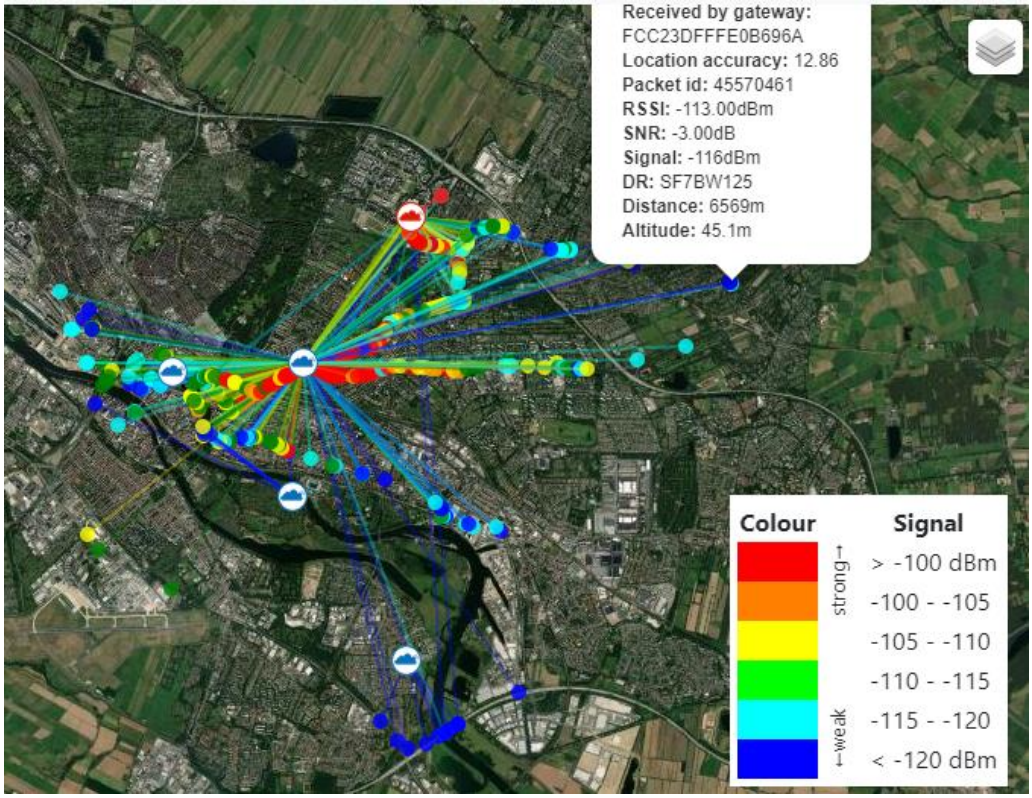

Fig. 20: Results taken by the TTN Mapper app for SF7

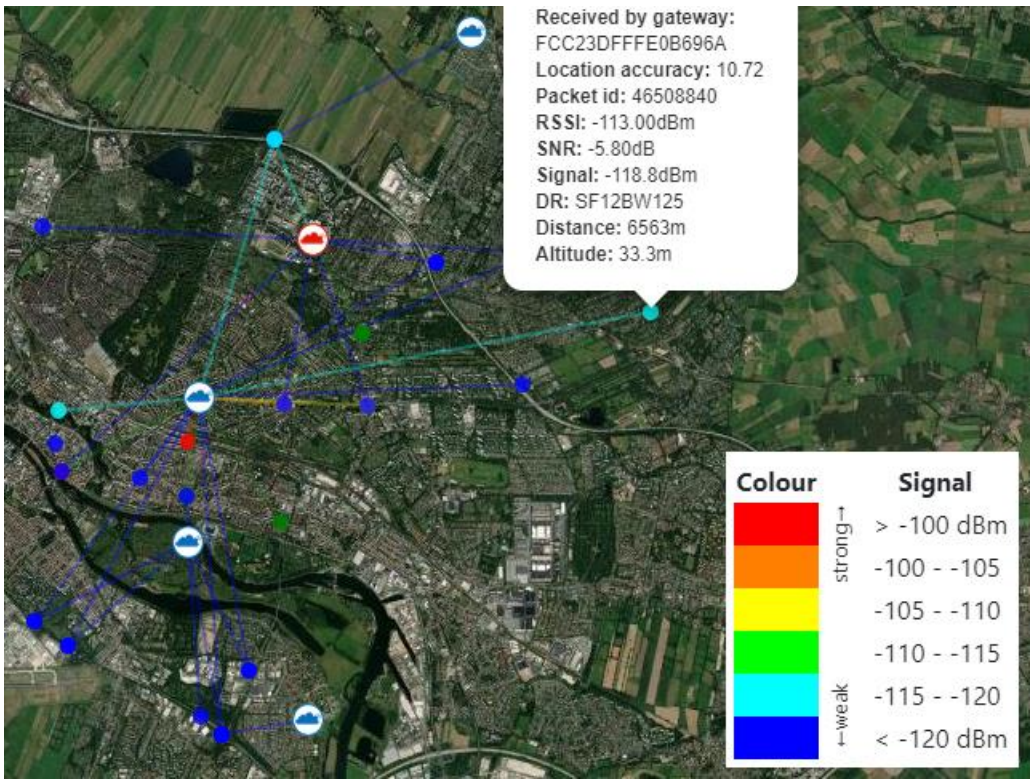

Fig. 21: Results taken by the TTN Mapper app for SF 12

Regarding the maximum coverage measured, the results were quite surprising if one compares to the maximum distances reported in the applications reviewed in chapter 2. What we found in this urban environment doubles those maximum measured ranges for rural areas in the Literature review.

During this scenario, various problems were encountered. Since in Bremen there are more than one GW in range, measuring the packet-loss ratio for different range intervals resulted problematic for a moving node. This is due to the fact that, within a distance of 200 m, for example, the node could find in range 2-3 different GWs and therefore, two consecutive packets could be at very different distances from the GW that received those packets.

It was also difficult to increase the distance from the GW without going out from the urban environment and therefore, the maximum coverage point measured might not be the highest coverage point existing.

3.3 Scenario 3: 2nd mobile setup

When the scenario 2 was proposed, we also wanted to measure the packet-loss ratio for different ranges from the GW, but due to the existence of many different GWs and the node connecting to many of them within a few meters, the idea was finally discarded for that scenario. Nevertheless, studying this packet-loss ratio behaviour was still interesting, and therefore this 3rd scenario was proposed.

Again, we are working on a mobile scenario, but this time not around the whole city of Bremen but in a straight line starting from the central GW that we saw on the previous scenario. To be able to move as straight as possible and to maintain relatively low speed, the node was installed this time on a bike instead of inside a car. Again, the TTN Mapper app for Android was used to track the position of the node and the SF 7 and 12 were tested in the same path three times each of them. The payload used was of again 50 bytes and the number of packets for SF 7 was of 1160 and for SF 12 of 36, i.e., the maximum number of packets allowed. The sending interval used for this scenario was the minimum allowed, once rounded up the decimal number. This means, for SF 7 the sending interval was of 3 s and for SF 12, of 82 s.

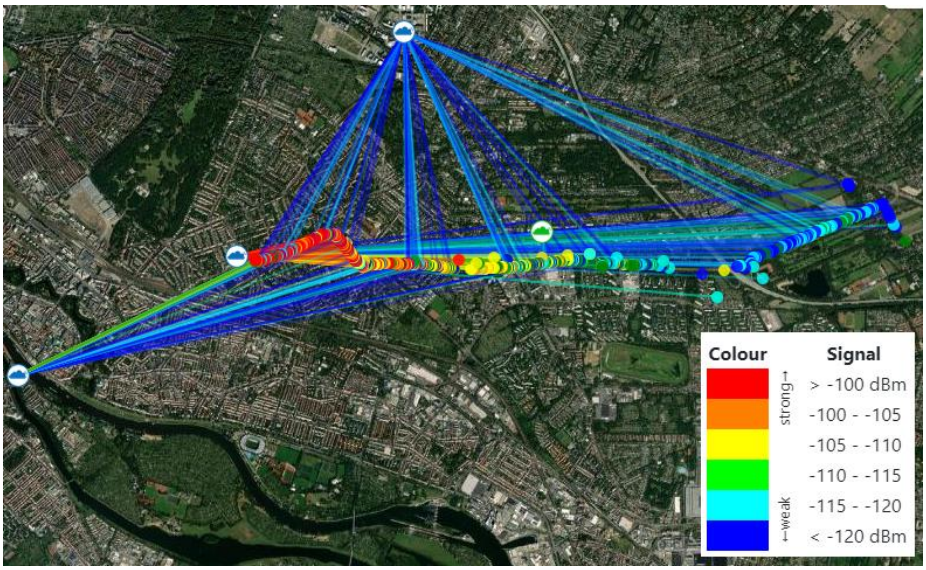

Fig. 22: results for SF 7 for scenario 3

In Fig. 22 and Fig. 23 it is shown the path followed for both cases, SF 7 and 12 respectively. As explained before, for this experiment we are going to focus only on the packets received by the central GW, so the second GW on the image starting from the left. This GW was elected since in the previous scenario it was shown as the predominant one. All packets not received by this GW will be stated as losses even if they were received by some other GW. The packet-loss ratio was measured for different ranges increasing in 500 m for SF 7, and increasing on 1 km for SF 12, from 0 m to 7 km. The results are shown in Table 8 and Table 9, where the ranges are expressed in km. Again, the mean of the packet-loss ratio was calculated as well as the deviation for each case.

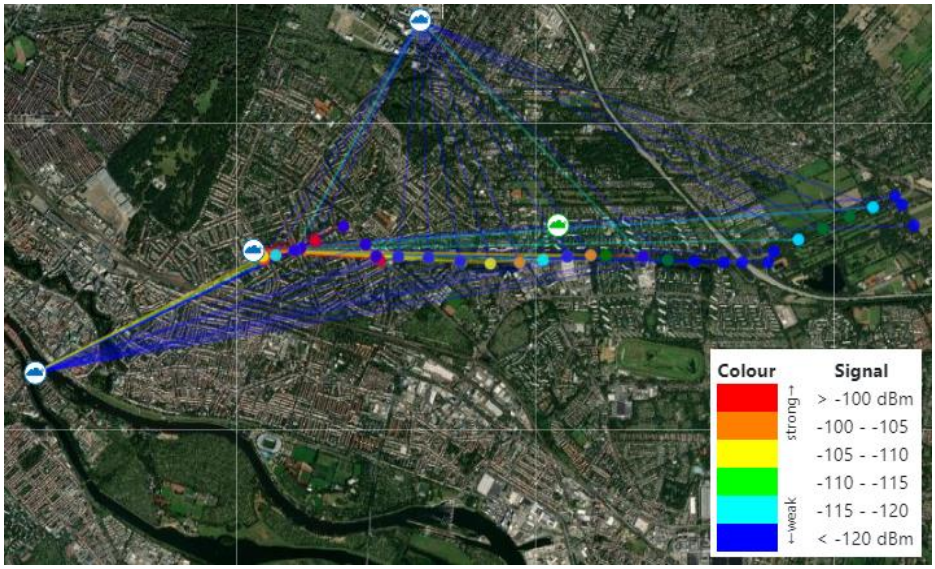

Fig. 23: results for SF 12 for scenario 3

Table 8: scenario 3 results for SF 7

SF 7		
Range (km)	$\overline{PL}$	**Deviation**
0-0.5	50.83%	0.110220
0.5-1	27.37%	0.082825
1-1.5	25.37%	0.162431
1.5-2	32.23%	0.127186
2-2.5	33.00%	0.057582
2.5-3	29.84%	0.087694
3-3.5	29.93%	0.042194
3.5-4	36.16%	0.096106
4-4.5	62.14%	0.179575
4.5-5	85.19%	0.066772
5-5.5	67.65%	0.083166
5.5-6	61.39%	0.152119
6-6.5	70.74%	0.060317
6.5-7	100.00%	0.000000
Total	49.63%	0.092134

Table 9: scenario 3 results for SF 12

SF 12		
Range (km)	$\overline{PL}$	**Deviation**
0-1	66.55 %	0.119541
1-2	68.89%	0.300617
2-3	34.92%	0.357407
3-4	19.44%	0.173472
4-5	19.44%	0.173472
5-6	0%	0.000000
6-7	37.78%	0.038490
Total	39.81%	0.084863

At this point it is convenient to remind that this experiment was only focusing on one GW. This means, the losses expressed in the tables correspond to all those packets that have not been received

by this exact GW but that might have been received by any other in range. The ranges for SF 12 were given in sets of 1 km instead of 500 m since, due to the sending interval (82 s) the number of packets every 500 m was too low, usually reduced to 0 when only accounting for the GW aforementioned. In any case, we see once again that the expected was reached: there are less losses for higher SF value. To properly evaluate in what percentage the losses decrease or increase depending on the range, a better setup would be one where the testers are able to use a private LoRa network. During this experiment it was also found that the maximum range between GW-node was of more of 7 km which once again exceeded the expectations we had.

Chapter 4: Mathematical model of the LoRa performance

This chapter aims to show how some parts of the LoRa properties can be mathematically described. Although the adoption of LoRa increases, there aren't many resources explaining analytically how LoRa works.

During the writing of this thesis, several equations describing LoRa were shown, and will be here summarized.

First, the formula describing the transmission delay was introduced in (4), and modified for our specific case (no CRC) in (5), here again presented:

$$D_{TX} = \left[20.25 + \left(\frac{28 - 4SF}{SF - 2O}\right) \cdot CR\right] \cdot \frac{2^{SF}}{BW} + \left[\left(\frac{8L}{SF - 2O}\right) \cdot CR\right] \cdot \frac{2^{SF}}{BW} \quad (5)$$

For deployments using LoRa and TTN, the limitations imposed on them, described in the sub-chapter 1.11 **Limitations**, have to be followed. Therefore, the minimum sending interval (*S*), or minimal time-off, should be calculated as introduced in (7), together with the maximum number of packets (N_{max}) allowed per day, in (6).

$$N_{max} = Floor(^{30}/_{ToA}) \quad (6)$$

$$S = \frac{ToA}{Duty\ Cycle} - ToA \quad (7)$$

Finally, the equation to calculate the bit-rate (R_b) depending on the SF and CR, is also shown in (1).

$$R_b = SF \cdot \frac{BW}{2^{SF}} \cdot CR\ [bits/s] \quad (1)$$

To be able to answer what is the power consumption for our device when using LoRa, the whole current consumption of the complete transmission should be tracked for example with an oscilloscope. With our experimental devices, it was not possible to measure the power consumption precisely because the multimeter we used could not record a complete transmission, but only the current used at a specific time, which could be extremely varying.

So, what can then be modelled? As it was shown in chapter 3, the expected delay for each SF value with different payload values can be calculated. Using it together with limitations from (6)and (7), the minimum transmission duration for the different SF values and for different payloads can also be modelled. If we talk about power consumption, with the proper instruments it should be easy to predict the power that will be consumed during a transmission, using either class A or C.

When knowing the parameters not only of the nodes used but of the GW, the path-loss model can be obtained, although it can always be applied to the specific environment only. Following this and the motivation of the thesis, it would be interesting to develop a path-loss model for urban environments from our collected data. To do this, however, sufficient information about the GW was not available. In any case, in the following sub-chapters one can find a brief summary of the theoretical approach of the general path-loss model for urban environments, as well as path-loss related approaches from [1] and [2], the second one being an example of the application of the path-loss model that could be derived from our experiments.

4.1 Path-loss model for urban environments

This sub-chapter will briefly introduce the path-loss model for urban environments extensively explained in [35]. It is included as a part of their chapter dedicated to large-scale path loss for mobile radio propagation. As the author explains, the models for propagation show that the average received signal power decreases logarithmically as described in equation (9), where *n* is the path-loss exponent, *d* is the distance between node and GW, and d_0 is the reference distance obtained from measurements close to the node. Therefore, $\overline{PL}(d_0)$ is the path-loss obtained for this reference distance, i.e., the path-loss reference.

$$\overline{PL}(dB) = \overline{PL}(d_0) + 10nlog(\frac{d}{d_0}) \tag{9}$$

The value of the path-loss exponent indicates in what measure the path-loss increases as the distance also increases. This means, *n* will have a larger value for environments with more interferences or obstacles. In Table 10 the typical path-loss exponent values for different environments are listed, although its exact value depends on the specific environment.

Table 10: Path-loss exponents for different environments [35]

Environment	**Path-loss exponent, *n***
Free space	2
Urban area cellular radio	2.7 to 3.5
Shadowed urban cellular radio	3 to 5
In building line-of-sight	1.6 to 1.8
Obstructed in building	4 to 6
Obstructed in factories	2 to 3

To calculate the path-loss reference, the free space path loss formula is used, given in (10); or through the measurements from distance d_0 as mentioned before.

$$PL(dB) = 10log\left(\frac{P_t}{P_r}\right) = -10\log(\frac{G_t G_r \lambda^2}{(4\pi)^2 d^2}) \tag{10}$$

Considering the environment conditions are also time variable, a modification on the previous equations is introduced in (11).

$$PL(d)[dB] = \overline{PL}(d) + X_\sigma = \overline{PL}(d_0) + 10nlog\left(\frac{d}{d_0}\right) + X_\sigma \tag{11}$$

Where X_σ is a zero mean Gaussian distributed random variable with standard deviation σ. This answers to the fact that it has been shown that, as the author says in [35], "at any value of *d*, the path loss *PL(d)* at a particular location is random and distributed log-normally about the mean distance dependent value." This is attributed to the shadowing effects and referred to as *log-normal shadowing*. Similarly to the path-loss exponent, σ is also computed from measured data using linear regression.

4.2 LoRaSIM

In this subchapter, we refer again to the work done in [1], where the authors developed a mathematical model of LoRa's link behaviour.

The aim of the authors is to model the communication range of LoRa, in dependence of the SF and the BW and the capture effect of LoRa transmissions depending on transmission timings and power.

First, they define the parameters to be used, included in Table 11.

Table 11:Parameters used in the model

Parameter name	Meaning
P_{rx}	received signal power in dB
S_{rx}	sensitivity threshold of the receiver
P_{tx}	transmit power in dB
G_{tx}	transmitter antenna gain in dBi
L_{tx}	transmitter loss in dB
L_{pl}	path loss in dB
L_m	miscellaneous losses in dB
G_{rx}	receiver antenna gain in dBi
L_{rx}	receiver losses

The approach proposed starts with equation (12), comparing the received power to that transmitted minus the losses along the transmission, plus the gain on the transmitter and receiver antenna; a rather straightforward proposal:

$$P_{rx} = P_{tx} + G_{tx} - L_{tx} - L_{pl} - L_m + G_{rx} - L_{rx} \tag{12}$$

To simplify, equation (12) can be reduced into equation (13):

$$P_{rx} = P_{tx} + GL - L_{pl} \tag{13}$$

Where *GL* represents a combination of all gains and losses, and L_{pl} represents the path loss, which is defined by the nature of the communication environment.

To describe the path loss, they use the log-distance model, commonly used for built-up environments modelling. Based on this, the path loss in dependence of the communication distance is described as:

$$L_{pl}(d) = \overline{L_{pl}}(d_0) + 10\gamma \log\left(\frac{d}{d_0}\right) + X_\sigma \tag{14}$$

Where $L_{pl}(d)$ is the path loss in dB, $\overline{L_{pl}}(d_0)$ is the mean path loss at the reference distance d_0, γ is the path loss exponent, and $X_\sigma \sim N(0, \sigma^2)$ the normal distribution with zero mean and σ^2 variance to account for shadowing. Authors call us on remembering that the communication range,

and therefore the exact path loss model is extremely dependent on the environment and due to that, a generic model cannot be given.

For sensitivity, they define equation (15) for a radio receiver at room temperature:

$$S = -174 + 10log_{10}(BW) + NF + SNR \quad (15)$$

Where the first term refers to thermal noise in 1 Hz of bandwidth and can only be influenced by changing the temperature of the receiver. BW is the bandwidth of the receiver, NF is the receiver noise figure (fixed) and SNR is the signal-to-noise ratio, determined by the SF. A higher SNR will be obtained for higher SF values, as mentioned before.

As the authors note, the sensitivity can increase or decrease by 3dB influenced by BW or SF. As the BW changes in steps of powers of 2, increasing the BW decreases the sensitivity by 3dB. On the other hand, increasing the SF doubles the chips per symbol, thus increasing the sensitivity by 3dB.

From equations (13), (14) and (15), it is possible to estimate whether a LoRa transmission will be received. It is described as:

$$R = \begin{cases} 1, & if P_{rx} < S_{rx} \\ 0, & if\ else \end{cases} \quad (16)$$

As they explain, to determine P_{rx}, the parameters $\overline{L_{pl}}$, d_0, γ and σ must be set and the distance d must be known. Furthermore, the value of S_{rx} is dependent on the BW and SF values used.

They also analyse if, given a collision between two LoRa transmissions, the receiver can decode the packets correctly or not. What determines this answer are CF, SF, transmission power and timing.

First, they define the interval where two packets overlap using the following equation:

$$O(x, y) = |m_x - m_y| < d_x + d_y \quad (17)$$

where m_i and d_i are respectively the midpoint of the reception interval (a_i,b_i) for a packet $i \in \mathbb{N}$ whose reception starts at a_i and ends at b_i, and the midpoint length.

$$m_i = \frac{a_i + b_i}{2} \quad (18)$$

$$d_i = \frac{b_i - a_i}{2} \quad (19)$$

Regarding CF, the authors claim that "when two transmissions overlap in time, but not in Carrier Frequency (CF), they do not interfere with each other and can both be decoded (assuming a receiver is listening at both carrier frequencies)." Given that, they define the collision of two transmissions on CF as:

$$C_{freq}(x, y) = \begin{cases} 1, & if\ |f_x - f_y| < f_{treshold} \\ 0, & else \end{cases} \quad (20)$$

Where f_x and f_y are the center frequencies of the transmissions x and y, and $f_{treshold}$ is the minimum tolerable frequency offset.

Moving on to the SF, the collision equation on SF is defined as:

$$C_{sf} = \begin{cases} 1, & if\ SF_x = SF_y \\ 0, & else \end{cases} \quad (21)$$

Where SF_x and SF_y are the SF of the transmissions x and y, respectively since, as already mentioned, two transmissions with different SF and the same CF and BW can be correctly decoded because different SF are orthogonal.

In regards of transmission power, the capture effect is mentioned. This effect occurs when a signal with the higher power supresses a weaker signal at the receiver. Therefore, the equation followed for collision in power is:

$$C_{pwr}(x,y) = \begin{cases} 1, & if\ (P_x - P_y) > P_{treshold} \\ 0, & else \end{cases} \quad (22)$$

Where P_x is the received signal strength of transmission x, P_y is that of transmission y and $P_{treshold}$ is the power threshold needed so one signal suppresses the other instead of making the receiver switch between the two, which happens when the power difference is too small.

For timing collision, the authors base the equation definition on an experiment from which they concluded that "the critical section of a packet reception starts at the last 5 preamble symbols" [1], redefining the interval transmission of x as in (23)with T_{sym} as the symbol time and N_{pp} as the number of programmed preamble symbols. Therefore, the collision of packet x with packet y takes place on the critical section x_{cs}, defined in (24) where the operator O refers to the function defined in (17).

$$x_{cx} = (a_x + T_{sym} \cdot (N_{pp} - 5), b_x) \quad (23)$$

$$C_{cs}(x,y) = \begin{cases} 1, & if\ O(x_{cs}, y) \\ 0, & else \end{cases} \quad (24)$$

Finally, the collision occurs when all previous equations (17) to (24) take place:

$$C(x,y) = O(x,y) \cap C_{freq}(x,y) \cap C_{sf}(x,y) \cap C_{pwr}(x,y) \cap C_{cs}(x,y) \quad (25)$$

4.3 Mobile LoRaWAN

Coming back to the testing carried out in [2], the authors developed a channel attenuation model based on their experimental results. Therefore, this model was derived only for one channel at 868.67 MHz, rather than for each individually. The model can be used, as the authors claim, in areas similar to Oulu to superficially estimate the communication distance when using LoRa.

First, they used the measured RSSI (received signal strength indicator) to calculate the path loss, PL:

$$PL = |RSSI| + SNR + P_{TX} + G_{RX} \quad (26)$$

Where P_{TX} is the Effective Isotropic Radiated Power (EIRP)[1], SNR and G_{RX} the receiver's antenna gain. From equation (26), the authors derived the expected path loss as:

$$EPL = B + 10nlog_{10}(^{d}/_{d_0}) \quad (27)$$

Where B is the path loss, n the path loss exponent, d is the distance between the node and the base station and d_0 is the 1 km reference distance. It is easy to see equation (27) follows a very similar approach to that in (14), proposed by the authors in [1]. Furthermore, authors in [2] also consider the standard deviation (std) of shadow fading, as also considered by the authors of LoRaSIM. As included in [2], this standard deviation describes a deviation between the measured path loss and the expected path loss, being calculated as:

$$\sigma_{sf} = std(PL - EPL) \quad (28)$$

In Fig. 24 and Fig. 25 we can observe the results obtained for an uplink connection on ground and on water. In Table 12, the calculated path loss exponents and intercepts for both cases are presented. As we can see, for the on-ground case, the path loss exponent is larger than the free space path loss exponent, which the author attribute to buildings and/or other obstacles which might have interfered signal propagation. Compared to the on-water results, where no obstacles were present, the path loss exponent remains below the exponent of the free space model, which further supports this theory.

Table 12: Channel characteristics [2]

	Measurement scenario		Free space
Metric	**Car**	**Boat**	
Path loss exponent (n)	2.32	1.76	2.00
Path loss intercept (B)	128.95	126.43	91.22
Shadow fading (σ_{sf})	7.8dB	8.0dB	-

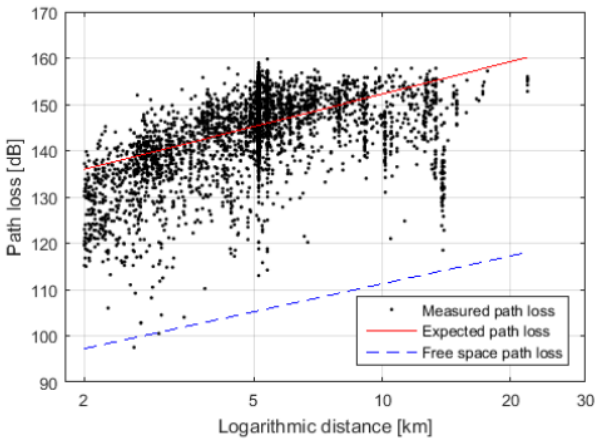

Fig. 24: Path loss for on-ground measurements [2]

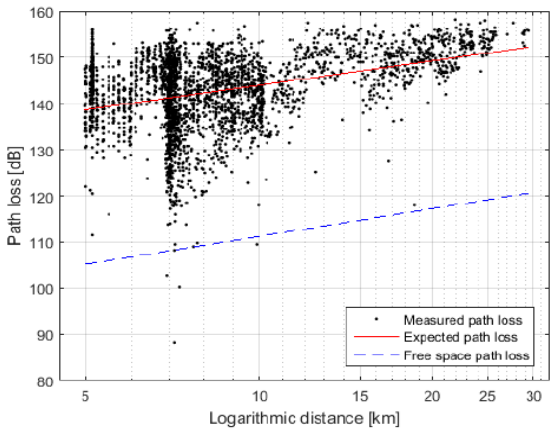

Fig. 25: Path loss for on-water measurements [2]

[1] "EIRP is Effective Isotropic Radiated Power, also called the Equivalent Isotropic Radiated Power. In antena measurements, the measured radiated power in a single direction is known as the EIRP. (…) It can also be thought of as the amount of power a perfectly isotropic antenna would need to radiate to achieve the measured value." [33]

Chapter 5: Conclusion

In this work, three main tasks were accomplished: first, to conduct an extensive Literature review to figure out IoT based scenarios with LoRa technology and determine relevant KPIs. Second, to conduct several experiments to understand how the identified KPIs behave under different parameter configuration; and third, to investigate how to model mathematically the LoRa performance.

Through the first chapter, the LoRa technology was introduced and summarised its configurable parameters. The second chapter discusses what kind of applications used LoRa and what kind of requirements they have, allowing us to identify the KPIs and the parameters influencing them. Also, we were able to select real-used values for the different parameters, which were introduced in chapter 3.

The third chapter consists of three different experimental scenarios: one static and two mobile. By means of the first scenario, we got to test the delay existing for all SF configurations together with different payload values, from 1 to 51. It was possible for us to see that the expected and obtained results presented a greater difference for increasing SF values. As expected, the delay for higher SF values and higher payload sizes was greater. The packet-loss ratio was also tested for the maximum number of packets allowed for each SF configuration, showing a higher packet-loss ratio for lower SF values.

Through the second and third scenarios, the packet-loss ratio was also analysed. In the second scenario, the node moved around the city obtaining different distances of node-GW and differently built-up environments, referring to density of buildings or their height. Again, the packet-loss ratio obtained for SF 7 was higher than the obtained for SF 12. Finally, the third scenario focused on a single GW, aiming to study the packet-loss ratio in increasing ranges. It was possible to observe a higher packet-loss ratio for SF 7 than for SF 12 in all ranges. Also, higher packet-loss ratio could be observed for lower distances of node-GW, which coincide with more dense areas of the city. In both scenarios 2 and 3, quite high maximal coverage ranges were observed, between 6.5 km to 7.2 km.

Finally, the current usage when using class A and C was also measured, allowing us to observe a higher usage for class C devices. Even so, due to lack of precise tools, the complete transmission could not be tracked in terms of current usage at every instant of time, which might have allowed us to define the power consumption for each case.

To conclude with the whole study, in chapter 4 we summarized the equations found to define or model some parts of LoRa. These included the equation to predict the delay of the transmission, depending on SF, BW, payload and CR. Also, the equations to calculate the maximum number of packets per day and minimum sending interval to comply with the limitations for LoRa. It was also mentioned that it could be interesting to develop the path-loss model for urban environments together with our results, but due to the lack of some parameters' details and the nature of our testing, i.e., we were not using a private network, it was not possible. Therefore, a brief theoretical approach of this model was presented, together with two papers that worked with this same model.

In summary, it is possible to claim that LoRa complies in general terms with what is theoretically expected, in regards to the change of its parameters and how it affects the communication. In any case, the performance gets greatly affected when changing the nodes from static to mobile positions. Depending on the nature of the application, LoRa might be considered not reliable

enough if the results of packet-loss ratio are considered, or too restrictive in terms of amount of data allowed to be sent, if we focus on the maximum payload allowed and the maximum number of packets permitted per day. About the range, the expectations were overcome, but the results might be highly dependent on the software used during the tests and on the specific setup of the environment tested.

Bibliography

[1] M. Bor, U. Roedig, T. Voigt and J. Alonso. 2016. Do LoRa low-power wide area networks scale? ***The 19th ACM International Conference on Modeling, Analysis and Simulation of Wireless and Mobile Systems*.**

[2] Petajajarvi, Juha, et al. 2015. On the coverage of LPWANs: range evaluation and channel attenuation model for LoRa technology. ***The 14th IEEE International Conference on ITS Telecommunications***, 55-59

[3] A. Augustin, J. Yi, T. Clausen, and W. Townsley. Sep. 2016. A Study of LoRa: Long Range & Low Power Networks for the Internet of Things ***Sensors***, vol. 16, no. 12, p. 1466.

[4] P. Neumann, J. Montavont, and T. Noel. 2016. Indoor deployment of low power wide area networks (LPWAN): A LoRaWAN case study. ***The 12th IEEE International Conference on Wireless and Mobile Computing, Networking and Communications***, 1–8.

[5] Gregora, Lukas, Lukas Vojtech, and Marek Neruda. 2016. Indoor signal propagation of LoRa technology. ***The 17th IEEE International Conference on Mechatronics-Mechatronika****, 1-4*.

[6] T. Petric, M. Goessens, L. Nuaymi, L. Toutain, and A. Pelov. 2016. Measurements, performance and analysis of LoRa FABIAN, a real world implementation of LPWAN. ***The 27th IEEE Annual International Symposium on Personal, Indoor, and Mobile Radio Communications,*** 1–7.

[7] D. H. Kim, J. Y. Lim, and J. D. Kim. 2016. Low-Power, Long-Range, High- Data Transmission Using Wi-Fi and LoRa. ***The 6th International Conference on IT Convergence and Security,*** 1–3.

[8] D. Bankov, E. Khorov, and A. Lyakhov. 2016. On the Limits of LoRaWAN Channel Access. ***The International Conference on Engineering and Telecommunication***,10–14.

[9] Ahlers, Dirk, et al. 2016. A measurement-driven approach to understand urban greenhouse gas emissions in Nordic cities. ***NIK***.

[10] F. Yang et al. 2016. PnP-WAN: Wide Area Plug and Play Sensing and Actuation with LoRa**.** ***The IEEE International SoC Design Conference***, 225–226.

[11] Tanumihardja, Wisena Aditya, and Edy Gunawan. 2015. On the application of IoT: Monitoring of troughs water level using WSN. ***IEEE Conference on Wireless Sensors***, 58-62

[12] F. Orfei, C. Mezzetti, and F. Cottone. 2016. Vibrations powered LoRa sensor: An electromechanical energy harvester working on a real bridge. **IEE *Sensors***, 1-3.

[13] A. M. Abu-Mahfouz et al. Realtime dynamic hydraulic model for potable water loss reduction. ***Procedia Eng***., vol. 154, no. 7, 99–106.

[14] Khutsoane, O., Isong, B., & Abu-Mahfouz, A. M. 2017. IoT devices and applications based on LoRa/LoRaWAN. ***IECON 2017-43rd Annual Conference of the IEEE Industrial Electronics Society***, 6107-6112.

[15] W. Zhao, S. Lin, J. Han, R. Xu and L. Hou. 2017. Design and Implementation of Smart Irrigation System Based on LoRa. ***2017 IEEE Globecom Workshops (GC Wkshps)***, 1-6.

[16] L. H. Trinh, V. X. Bui, F. Ferrero, T. Q. K. Nguyen and M. H. Le. 2017. Signal propagation of LoRa technology using for smart building applications. ***2017 IEEE Conference on Antenna Measurements & Applications (CAMA),*** 381-384.

[17] J. Petäjäjärvi, K. Mikhaylov, M. Hämäläinen and J. Iinatti. 2016. Evaluation of LoRa LPWAN technology for remote health and wellbeing monitoring. ***2016 10th International Symposium on Medical Information and Communication Technology (ISMICT),*** 1-5.

[18] M. Rizzi, P. Ferrari, A. Flammini and E. Sisinni. 2017. Evaluation of the IoT LoRaWAN Solution for Distributed Measurement Applications. ***IEEE Transactions on Instrumentation and Measurement***, vol. 66, no. 12, 3340-3349.

[19] A. Bhawiyuga, K. Amron, R. Primanandha, D. P. Kartikasari, H. Arijudin and D. A. Prabandari. 2019. LoRa-MQTT Gateway Device for Supporting Sensor-to-Cloud Data Transmission in Smart Aquaculture IoT Application. ***2019 International Conference on Sustainable Information Engineering and Technology (SIET),*** 187-190.

[20] L. Li, J. Ren and Q. Zhu. 2017. On the application of LoRa LPWAN technology in Sailing Monitoring System. ***13th Annual Conference on Wireless On-demand Network Systems and Services (WONS),***. 77-80.

[21] K. Mikhaylov, J. Petäjäjärvi, and T. Hänninen. 2016. Analysis of Capacity and Scalability of the LoRa Low Power Wide Are Network Technology. ***European Wireless 2016; 22th European Wireless Conference.*** 119-124.

[22] D. Singh, O. G. Aliu, and M. Kretschmer. 2018. LoRa WanEvaluation for IoT Communications. ***2018 International Conference on Advances in Computing, Communications and Informatics (ICACCI)***. 163-171.

[24] J. Haxhibeqiri, E. De Poorter, I. Moerman, and J. Hoebeke. 2018. A survey of LoRaWAN for IoT: From technology to application. ***Sensors,*** 18(11), 3995.

[25] The Things Network. 2020, Nov. LoRaWAN Frequency Plans and Regulations by Country. ***Available on:*** https://www.thethingsnetwork.org/docs/lorawan/frequencies-by-country.html

[26] The Things Network. 2020, Nov. Frequency plan. ***Available on:*** https://www.thethingsnetwork.org/docs/lorawan/frequency-plans.html

[27] LoRa® Alliance Technical Marketing Workgroup. 2015. LoRaWAN™ What is it? A technical overview of LoRa® and LoRaWAN™. ***LoRa® Alliance.*** 4.

[28] The Things Network. 2020, Nov. Classes. ***Available on:*** https://www.thethingsnetwork.org/docs/lorawan/classes.html

[29] The Things Network. 2020, Nov. LoRaWAN Architecture. ***Available on:*** https://www.thethingsnetwork.org/docs/lorawan/architecture.html

[30] The Things Network. 2020, Dec. LoRaWAN airtime calculator. ***Available on:*** https://www.thethingsnetwork.org/airtime-calculator

[31] The Things Network. 2020, Dec. LoRaWAN Adaptative Data Rate. ***Available on:*** https://www.thethingsnetwork.org/docs/lorawan/adaptive-data-rate.html

[32] The Things Network. 2020, Dec. Duty cycle. ***Available on:*** https://www.thethingsnetwork.org/docs/lorawan/duty-cycle.html

[33] Antenna-Theory.com. 2021, Jan. Effective Isotropic Radiated Power (EIRP). ***Available on:*** https://www.antenna-theory.com/definitions/eirp.php

[34] TTN Mapper app for Android. 2021, April. ***Available on:*** https://play.google.com/store/apps/details?id=org.ttnmapper.phonesurveyor&hl=es&gl=US

[35] T. S. Rappaport et al. 1996. Wireless communications: principles and practice, volume 2. ***Prentice Hall PTR***. 102 – 107.